Journal of Marine Research, 73, 71–92, 2015

Nitrogen substrate–dependent nitrous oxide cycling in salt marsh sediments

by Qixing Ji[1], Andrew R. Babbin[2], Xuefeng Peng[3], Jennifer L. Bowen[4], and Bess B. Ward[5]

ABSTRACT

Nitrous oxide (N_2O) is important to Earth's climate because it is a strong absorber of radiation and an important ozone depletion agent. Increasing anthropogenic nitrogen input into the marine environment, especially to coastal waters, has led to increasing N_2O emissions. Identifying the nitrogen compounds that serve as substrates for N_2O production in coastal waters reveals important pathways and helps us understand their control by environmental factors. In this study, sediments were collected from a long-term fertilization site in Great Sippewissett Marsh, Falmouth, Massachusetts. The ^{15}N tracer incubation time course experiments were conducted and analyzed for potential N_2O production and consumption rates. The two nitrogen substrates of N_2O production, ammonium and nitrate, correspond to the two production pathways, nitrification and denitrification, respectively. When measurable nitrate was present, despite ambient high ammonium concentrations, denitrification was the major N_2O production pathway. When nitrate was absent, ammonium became the dominant substrate for N_2O production, via nitrification and coupled nitrification-denitrification. Net N_2O consumption was enhanced under low oxygen and nitrate conditions. N_2O production and consumption rates increased with increasing levels of nitrogen fertilization in long-term experimental plots. These results indicate that increasing anthropogenic nitrogen input to salt marshes can stimulate sedimentary N_2O production via both nitrification and denitrification, whereas episodic oxygen depletion results in net N_2O consumption.

Keywords. Nitrous oxide, nitrogen substrate, nitrification, denitrification, salt marsh, sediment, long-term fertilization, ^{15}N tracer

1. Department of Geosciences, Princeton University, Princeton, NJ 08540. ***e-mail: qji@princeton.edu***

2. Department of Geosciences, Princeton University, Princeton, NJ 08540; and Department of Civil and Environmental Engineering, Massachusetts Institute of Technology, Cambridge, MA 02139. ***e-mail: babbin@mit.edu***

3. Department of Geosciences, Princeton University, Princeton, NJ 08540. ***e-mail: xpeng@princeton.edu***

4. Biology Department, University of Massachusetts at Boston, 100 Morrissey Blvd., Boston, MA 02125. ***e-mail: jennifer.bowen@umb.edu***

5. Department of Geosciences, Princeton University, Princeton, NJ 08540. Corresponding author: ***e-mail: bbw@princeton.edu***

1. Introduction

Nitrous oxide (N_2O) is a trace gas that has a strong greenhouse effect and is a powerful ozone depletion agent, with increasing emissions since the Industrial Revolution (Crutzen 1970; Cicerone 1987). Present-day N_2O concentration in the atmosphere is the highest it has been in the past 800,000 years (Schilt et al. 2010; Intergovernmental Panel on Climate Change [IPCC] 2013). With control of CFCs accomplished by the Montreal Protocol, N_2O is likely to be the single most important anthropogenic ozone-depleting agent emitted in the 21st century (Ravishankara, Daniel, and Portmann 2009).

Globally, more than 80% of total N_2O emissions can be attributed to microbial activities occurring in soil, open ocean, and coastal waters (IPCC 2013). Two microbial processes are the known major pathways for N_2O production. N_2O can be produced as a by-product during aerobic ammonium (NH_4^+) oxidation to nitrate (NO_3^-) by bacteria (Arp and Stein 2003) and archaea (Santoro et al. 2011). The other is denitrification, a stepwise reduction from NO_3^- that emits N_2O as a free intermediate in the absence of oxygen. Thus, NH_4^+ and NO_3^- are two nitrogen substrates for N_2O production. Generally, NH_4^+ is derived from organic nitrogen mineralization, whereas NO_3^- is the product of nitrification, and the substrate for subsequent denitrification. Increasing anthropogenic nitrogen supply into coastal waters has led to excess NH_4^+ and NO_3^-, which are intercepted and removed by coastal wetlands and sediments at the interface between land and sea. The biological removal of excess NH_4^+ and NO_3^- produces N_2O. Bange, Rapsomanikis, and Andreae (1996) estimated that coastal waters contribute up to 60% of global oceanic N_2O emissions. Salt marshes, situated in coastal areas, are "hot spots" of N_2O emission (Blackwell, Yamulki, and Bol 2010; Moseman-Valtierra et al. 2011).

Salt marshes are characterized by temporal and spatial variation of inorganic nitrogen (Brin et al. 2010) and oxygen availabilities (Howes et al. 1981). These two factors, combined with increasing nitrogen loading, regulate the magnitude and pathways of N_2O production. Determining the relative contribution of NH_4^+ and NO_3^- to N_2O production can help us evaluate the relative importance of nitrification and denitrification to N_2O emissions in the environment. Oxygen critically affects N_2O production and consumption because (1) N_2O production via NH_4^+ oxidation requires molecular oxygen; (2) N_2O production from NO_3^- and N_2O consumption are able to proceed only under low and zero oxygen; and (3) the enzyme that mediates N_2O consumption, nitrous oxide reductase (N_2OR), is the most oxygen-sensitive in the canonical denitrification pathway (Bonin, Gilewicz, and Bertrand 1989; Körner and Zumft 1989). Finally, N_2O emissions from salt marshes are expected to increase as a result of increasing anthropogenic nitrogen loading to coastal waters, as demonstrated by modeling and by nutrient enrichment experiments (Seitzinger and Kroeze 1998; Moseman-Valtierra 2012 and reference therein). Because of their natural gradients of oxygen and nitrogen concentrations, salt marshes are important experimental sites for studying N_2O production pathways and the effects of changing environmental conditions.

To investigate the effects of nutrient enrichment on salt marsh ecosystems, a long-term fertilization project was initiated in the 1970s in the Great Sippewissett Marsh, Falmouth, Massachusetts, by Valiela, Teal, and Sass (1973) and has been maintained without interruption. The results of long-term fertilization have included increases in aboveground biomass (Valiela, Teal, and Sass 1975; Howes, Dacey, and Goehringer 1986), loss of *Spartina alterniflora* and an increase in *Distichlis spicata* (Fox, Valiela, and Kinney 2012), and the alteration of microbial communities in high-nutrient environments (Hamlett 1986; Bowen et al. 2013). In addition, elevated rates of denitrification (Koop-Jakobsen and Giblin 2010; Kinney and Valiela 2013) and coupled nitrification-denitrification (Hamersley and Howes 2005) were associated with increasing fertilization.

In this study, biological N_2O production and consumption in the Great Sippewissett Marsh sediments were investigated using ^{15}N tracer incubation methods. Sediment NH_4^+ and NO_3^- were enriched with ^{15}N, and the rates of $^{15}NH_4^+$ and $^{15}NO_3^-$ transformation to N_2O were monitored over 8-hour incubations. The time courses were analyzed to determine potential rates of N_2O production and to determine relative contributions of NH_4^+ and NO_3^- as substrates for N_2O production. Furthermore, the effects of environmental factors, such as dissolved inorganic nitrogen availability, oxygen level, and fertilization level, on N_2O production rates and the relative contribution of NH_4^+ and NO_3^- were investigated.

2. Methods

a. Site description and fieldwork

Sediment samples were collected from the Great Sippewissett Marsh located in Falmouth, Massachusetts (41°35′3.1″ N, 70°38′17.0″ W). Circular plots (10 m radius) of the marsh have been fertilized biweekly during the growing season (late April to early November, ~20 weeks) without interruption since the early 1970s, using commercially available pelletized sewage sludge fertilizer (6% by weight total nitrogen, 0.9% NO_3^--N, 0.2% NH_4^+-N; Milorganite, Milwaukee, WI). The fertilizer is applied at three levels (Table 1) to each set of replicate plots: low fertilization (LF), high fertilization (HF), and extrahigh fertilization (XF). Two additional plots are not directly fertilized above background and serve as controls (C). The plots are located within an area of 0.48 km^2, where averaged weekly background nitrogen loading from precipitation is estimated to be 0.023 g N m^{-2} $week^{-1}$ (1.6 mmol N m^{-2} $week^{-1}$) (Bowen and Valiela 2001). Nitrogen loading from nitrogen fixation plus groundwater flow was 0.16 g N m^{-2} $week^{-1}$ (11 mmol N m^{-2} $week^{-1}$) (Valiela and Teal 1979). At the time of sampling, the dominant vegetation cover in C, LF, and HF plots was short-form *S. alterniflora* in the high marsh and tall-form *S. alterniflora* in the low marsh. Low marsh in the XF plots was also dominated by tall-form *S. alterniflora* (XF-t). High marsh in the XF plots was dominated by *D. spicata* (XF-d) mixed with small patches of short-form *S. alterniflora* (XF-m). See Fox, Valiela, and Kinney (2012) for detailed maps of vegetation cover.

Table 1. Physical and chemical properties of sediment samples, including initial ^{15}N percentage label for $^{15}N\text{-}NH_4^+$ treatment and $^{15}N\text{-}NO_3^-$ treatments. The concentrations of NH_4^+, NO_3^-, and N_2O in sediment are normalized to one gram of wet sediment. Standard deviations of measurements (n = 3) are shown in parentheses. The "n.d." represents below detection [NO_3^-] in samples; therefore, ^{15}N content of NO_3^- could not be determined (represented as "-"). *Equivalent fertilizer loading in the unit of mmol-N m^{-2} wk^{-1}

Plot	C	XF	C	LF	HF	XF	XF-m	XF-t	XF-d	C	HF	XF
Collection time	August 2012		November 2012							August 2013		
Fertilizer dosage	0	7.8	0	0.9	2.6	7.8	7.8	7.8	7.8	0	2.6	7.8
(g N m^{-2} $week^{-1}$)		560*		64*	190*	560*	560*	560*	560*		190*	560*
Moisture content	80.6	76.9	82.1	85.0	79.7	76.5	77.8	78.5	77.6	82.4	83.3	77.7
(% total weight)	(0.3)	(0.1)	(0.1)	(0.1)	(0.2)	(0.4)	(0.2)	(0.3)	(0.1)	(0.2)	(0.4)	(0.3)
N_2O (nmol g^{-1})	0.48	4.30	0.77	0.66	0.85	36.8	44.2	5.14	177	0.37	1.11	104
	(0.08)	(0.27)	(0.09)	(0.10)	(0.17)	(4.1)	(7.4)	(0.51)	(16)	(0.15)	(0.19)	(25)
NH_4^+ (nmol g^{-1})	270	263	1,030	1,730	1,810	1,230	3,710	726	2,920	72	330	1,040
	(14)	(12)	(73)	(110)	(150)	(15)	(93)	(180)	(230)	(12)	(26)	(37)
NO_3^- (nmol g^{-1})	4.2	7.5	n.d.	n.d.	n.d.	600	630	3.1	540	7.2	3.1	210
	(1.0)	(1.0)				(70)	(110)	(0.5)	(40)	(0.1)	(0.1)	(30)
$^{15}N\text{-}NH_4^+$ (%)	0.419	0.420	0.423	0.402	0.400	0.415	0.385	0.446	0.390	7.96	2.13	0.94
	(0.052)	(0.046)	(0.071)	(0.064)	(0.083)	(0.012)	(0.025)	(0.248)	(0.079)	(0.17)	(0.079)	(0.036)
$^{15}N\text{-}NO_3^-$ (%)	0.367	0.367	–	–	–	0.387	0.386	0.380	0.386	0.473	0.375	0.398
	(0.002)	(0.003)				(0.004)	(0.001)	(0.002)	(0.003)	(0.002)	(0.002)	(0.001)

Sediment cores were collected in August 2012, November 2012, and August 2013 so that N_2O dynamics could be examined in summer and late autumn. The plots where sediments were collected during each trip are listed in Table 1. Three to four sediment cores, representing both high and low marsh habitat and primary plant types, were collected from C, LF, HF, and XF plots. After the roots were carefully removed, sediments from the same plot were homogenized, and subsamples were used for incubation. Therefore, the sediments do not represent N_2O production for a particular habitat but, to a certain extent, the entire fertilized or control plot as a whole. Such an experimental design minimized the effects of small-scale heterogeneity in this complex environment. Additionally, in November 2012, sediments representing different vegetation cover were collected from one of the XF plots. Sampling was performed at daytime low tide when the marsh bed was above water. Approximately 15 cm deep sediment cores were collected using 30 cm long, 7 cm diameter acrylic tubes with a sharpened edge. Butyl stoppers and rubber caps were used to seal the top and bottom of the acrylic tube storing intact sediment. The intact cores were kept in coolers with frozen reusable ice gel packs (Techni Ice, Frankston, VIC, Australia) for no more than 72 hours before conducting incubations.

b. Sediment incubations

Replicate sediment cores taken from the upper 10 cm of the same fertilized plots were homogenized and aliquotted (15 $\pm$ 0.2 g) into preweighed 30 mL amber serum bottles (Wheaton, Millville, NJ). The bottles were sealed with butyl rubber stoppers and aluminum seals (National Scientific, Rockwood, TN). Two sets of tracer amendments (5 mL injection) were applied. The $^{15}N\text{-}NH_4^+$ treatments received ^{15}N-labeled NH_4Cl (99%; Cambridge Isotope Laboratories, Tewksbury, MA) and natural abundance KNO_3 (Fisher Scientific, Pittsburgh, PA). The $^{15}N\text{-}NO_3^-$ treatments received ^{15}N-labeled KNO_3 (99%; Cambridge Isotope Laboratories) and natural abundance NH_4Cl (Fisher Scientific). The initial ^{15}N labeling for NH_4^+ and NO_3^- was usually <1% (Table 1). For NH_4^+, the fraction of substrate ^{15}N labeling was calculated, assuming the ^{15}N content of the ambient NH_4^+ in sediment to be close to natural abundance ($^{15}N/^{14}N = 0.37\%$). The ^{15}N labeling for NO_3^- was measured using the denitrifier method (Sigman et al. 2001). After the tracer solution was added, the bottles were vortexed with glass beads to distribute the tracers in the sediment. Incubations were performed under atmospheric oxygen headspace in order to simulate the surface sediment conditions because oxygen is likely to penetrate along with root matrices down to 10 cm. Incubation experiments lasted 6 to 8 hours at room temperature (22°C), during which triplicate samples were sacrificed every 2 hours by adding 1 mL of 7 M $ZnCl_2$ to terminate biological activity.

A subset of XF sediments from November 2012 incubated under helium headspace was compared with incubations of the same sediment under an oxygenated headspace in order to investigate the effect of oxygen on N_2O production and consumption. The headspace of the incubation bottles was adjusted to a lower oxygen level by purging with ultrahigh-purity

helium at 4 psi for 20 minutes. After oxygen adjustment, the sediments were incubated, and inorganic nitrogen concentrations were measured in triplicate bottles sacrificed every 2 hours by adding 1 mL of 7 M $ZnCl_2$.

c. Analytical methods

Sediment moisture content was determined from the difference between wet and dry weight after drying sediment samples at 65°C to constant weight. NH_4^+ and NO_3^- were extracted from sediments using 2 M KCl after N_2O had been measured in the headspace. Slurries were placed on a reciprocal shaker for 30 minutes at 300 rpm, followed by centrifugation at 4,000g. The supernatant was filtered (pore size 0.2 μm) and then frozen at −20°C until analysis. NH_4^+ concentration was measured colorimetrically in triplicate using the phenol-hypochlorite method (Strickland and Parsons 1968); for 1 mL sample size, the detection limit was 0.5 μM. Samples with NH_4^+ concentrations exceeding 50 μM and 500 μM were diluted 10- and 20-fold with 2 M KCl, respectively. Absorbance was measured on a UV-1800 UV-Visible Spectrophotometer (Shimadzu, Kyoto, Japan). NO_3^- concentration was measured using a hot (90°C) acidified vanadium (III) reduction column coupled to a Teledyne Chemiluminescence NO/NOx Analyzer (Model 200E) (Garside 1982; Braman and Hendrix 1989). Samples (20–100 μL) were injected in triplicate, with a detection limit of 0.1 μM.

Prior to headspace N_2O analysis, the serum bottle was vortexed so that N_2O in the sediment was equilibrated with the headspace. Thus, when N_2O was extracted from the headspace, it was considered to represent the concentration and isotopic composition of N_2O in the sediment. N_2O was extracted from the headspace using a 1 mL (XF samples) or 3 mL (C, LF, and HF samples) plastic syringe (BD Biosciences, San Jose, CA). Concentrations of N_2O in August and November 2012 were measured by electron capture gas chromatography (GC-8A; Shimadzu). The detection limit was 2 pmol N (25°C, 1 atm). N_2O concentrations for samples from August 2013 were measured by mass spectrometry (Delta V Plus; Thermo Scientific, Waltham, MA), with a detection limit of 0.1 nmol N. N_2O $^{15}N/^{14}N$ isotopic ratio (denoted as ^{15}N-N_2O hereafter) was measured using mass spectrometry. Calibration standards for N_2O isotopic ratio, ranging from 0.37 to 1.74 ^{15}N atom %, were prepared according to the denitrifier method (Sigman et al. 2001), assuming complete conversion of KNO_3 with known $^{15}N/^{14}N$ isotopic ratio.

The total amount of each nitrogen species was normalized to unit wet weight of sediment. Results were reported as nanomoles per gram of wet homogenized sediment (nmol N g^{-1}). This unit is equivalent to micromoles per liter, assuming the density of the sediment slurry was close to that of water. In the same manner, the N_2O production and consumption rates are reported as nanomoles per gram of wet homogenized sediment per hour (nmol N g^{-1} h^{-1}). Such normalization on a mass basis rather than volume facilitated the computation of nitrogen transformation rates for comparison across different sediments.

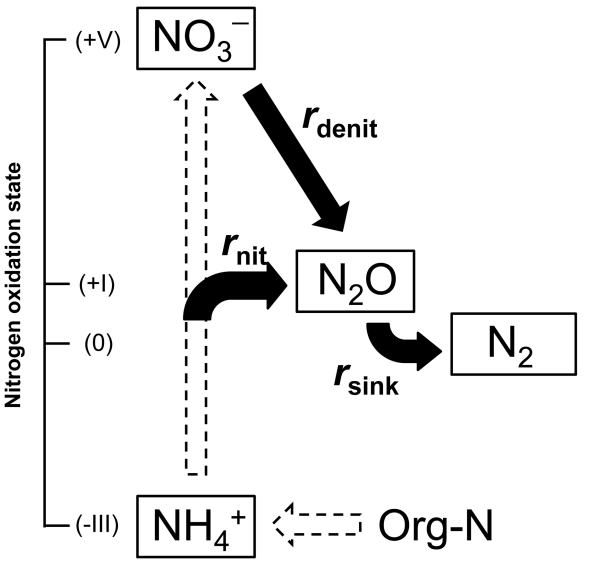

Figure 1. Conceptual model demonstrating nitrogen transformations involved in N_2O production and consumption. Reactions rates r_{nit}, r_{denit}, and r_{sink} indicate N_2O production from NH_4^+, N_2O production from NO_3^-, and N_2O consumption rates, respectively. Rates are all reported as nmol N g^{-1} h^{-1}. Dashed arrows indicate important processes supplying NH_4^+ and NO_3^-.

d. Model estimation of N_2O production and consumption rates

Based on mass balance, a box model (Fig. 1) representing the processes of N_2O production from NH_4^+ (r_{nit}) and NO_3^- (r_{denit}) and N_2O consumption (r_{sink}) was developed. NH_4^+ and NO_3^- were the two major dissolved inorganic nitrogen species because NO_2^- was below detection. Both NH_4^+ and NO_3^- were considered as possible nitrogen substrates for N_2O. Even in incubations in the presence of atmospheric oxygen, significant decreases in N_2O concentration were observed; therefore, consumption of N_2O was also considered. Defined as the ratio of ^{15}N over ^{14}N transformation rates for a specific process, isotope effects (α) associated with N_2O production from NH_4^+ (α_{nit}), production from NO_3^- (α_{denit}), and N_2O consumption (α_{sink}) were taken into account because the amended isotope comprised a very small fraction of the overall nitrogen pool. According to the compilations by Pérez (2005) and Dawson and Siegwolf (2007), isotope effects associated with N_2O production from NH_4^+ ranged from 0.932 to 0.965, production from NO_3^- ranged from 0.97 to 0.99, and N_2O consumption ranged from 0.996 to 0.987 in pure culture, soil, and aqueous samples. The values of α_{nit}, α_{denit}, and α_{sink} in the model simulations were fixed at 0.96, 0.98, and 0.99, respectively. In the case of XF sediment from November 2012, varying the values of α_{nit}, α_{denit}, and α_{sink} by 0.03, 0.01, and 0.01, respectively, the percent changes in rates relative to the base case were $<43\%$, and generally $<30\%$, which fell within the standard

Table 2. Descriptions of parameters used in numerical simulations.

Parameter	Description	Unit
r_{nit}	Rate of N_2O production from NH_4^+	nmol N g^{-1} h^{-1}
r_{denit}	Rate of N_2O production from NO_3^-	nmol N g^{-1} h^{-1}
r_{sink}	Rate of N_2O consumption	nmol N g^{-1} h^{-1}
α_{nit}	Nitrogen fractionation factor for r_{nit}	Unitless, 0.96
α_{denit}	Nitrogen fractionation factor for r_{denit}	Unitless, 0.98
α_{sink}	Nitrogen fractionation factor for r_{sink}	Unitless, 0.99
N_2O	Sediment N_2O concentration	nmol N g^{-1}
$\frac{^{15}NH_4^+}{^{14}NH_4^+}$	NH_4^+ ^{15}N content	%
$\frac{^{15}NO_3^-}{^{14}NO_3^-}$	NO_3^- ^{15}N content	%
$\frac{dN_2O}{dt}$	Change of N_2O concentration with time	nmol g^{-1} h^{-1}
$d\frac{\left(\frac{^{15}N_2O}{^{14}N_2O}\right)}{dt}$	Change of N_2O ^{15}N content with time	% h^{-1}

deviations of the Monte Carlo simulations. These approximations will serve as a starting point for future in-depth investigation for isotope effects associated with N_2O production and consumption in salt marshes.

The N_2O production and consumption rates were prognostically modeled in MATLAB using equations (1) and (2), assuming constant rates during the incubation (see Table 2 for descriptions of parameters).

$$\frac{dN_2O}{dt} = 0.5 \cdot (r_{nit} + r_{denit} - r_{sink}) \tag{1}$$

$$\frac{d(^{15}N_2O/^{14}N_2O)}{dt} \simeq \frac{1}{[N_2O]} \cdot \frac{^{15}N_2O}{^{14}N_2O} \cdot 0.5 \cdot (-r_{sink} \cdot \alpha_{sink} - r_{nit} - r_{denit} + r_{sink}) + \frac{1}{[N_2O]} \cdot 0.5 \cdot \left(r_{nit} \cdot \alpha_{nit} \cdot \frac{^{15}NH_4}{^{14}NH_4} + r_{denit} \cdot \alpha_{denit} \cdot \frac{^{15}NO_3}{^{14}NO_3}\right) \tag{2}$$

Equation (1) assumes a mass balance on N_2O concentrations controlled by rates of production and consumption. Equation (2) describes the control of ^{15}N-N_2O by rates of production and consumption, the ^{15}N atom % of NH_4^+ and NO_3^-, and the isotope effects involved in N_2O production and consumption.

Model inputs are ^{15}N content of NH_4^+ and NO_3^-, and ^{15}N-N_2O measured at each time point. A grid search was performed for r_{nit}, r_{denit}, and r_{sink} whereby the cost function was the mean-squared residual between the measured and the modeled values from N_2O concentration and isotope values from ^{15}N-NO_3^- and ^{15}N-NH_4^+ treatments. The inverse of the standard deviation of the residual between modeled results and measurements was used as a weighting coefficient to normalize each cost component to similar magnitudes (see supplementary material available online). By assigning initial conditions listed in Table 2 and calculating the minimum cost function, the N_2O production rate from NH_4^+ (r_{nit}) and NO_3^- (r_{denit}) and N_2O consumption (r_{sink}) were determined. To assess errors associated with modeled rates, a Monte Carlo simulation (n = 10,000) was run for each incubation; the simulations were generated from Gaussian distributions with the same mean and variance as the measured data set.

3. Results

a. Sediment characteristics

Sediments collected from the top 10 cm of the marsh changed color with depth, from dark brown to black. Root matrices penetrated deeper than 10 cm, with C and XF sediment having the most (65% weight to weight ratio [w/w]) and least (26% w/w) vegetative materials. After the stems and roots of marsh vegetation were removed and the remaining sediment was homogenized, pore water content averaged ~80% by weight (Table 1).

NH_4^+ concentration, in most cases, increased with fertilization level and in all plots exceeded NO_3^- concentration. Within the same fertilized plot, NH_4^+ concentrations in August were generally lower than in November (Table 1). NO_3^- concentrations were similar among C, LF, and HF plots, usually <8 nmol g^{-1}, but were two orders of magnitude higher (>500 nmol g^{-1}) in XF, XF-m, and XF-d sediment. In November 2012, XF-m and XF-d had >500 nmol N g^{-1} NO_3^-, whereas XF-t had <5 nmol N g^{-1} NO_3^-. The homogenized XF sediment (XF) consisted of 45% (w/w) of XF-m, 38% of XF-t, and 17% of XF-d and had NO_3^- concentrations of ~600 nmol N g^{-1}. Nitrite was not detected in any sediment samples. NH_4^+ plus NO_3^- increased with increasing fertilization (Table 1). N_2O concentrations were similar (<1.2 nmol g^{-1}) in C, LF, and HF sediment ,whereas XF sediment had elevated N_2O concentrations ranging from 4.3 nmol g^{-1} in August 2012 to 177.3 nmol g^{-1} in XF-d in November 2012.

b. Change of inorganic nitrogen with time during incubations of C and XF

The greatest contrast in the biogeochemistry in the salt marsh was observed between C and XF plots (Fig. 2); therefore, results from C and XF incubations are the focus of Sections 3b and c (for the complete data set, see Fig. S1 in the supplementary material). NH_4^+ concentrations in C incubations from November 2012 and August 2013 did not change significantly ($P = 0.18$ and 0.88, respectively, analysis of variance [ANOVA]) during the 8-hour incubation. XF sediments collected in August 2013 were the only incubation in which

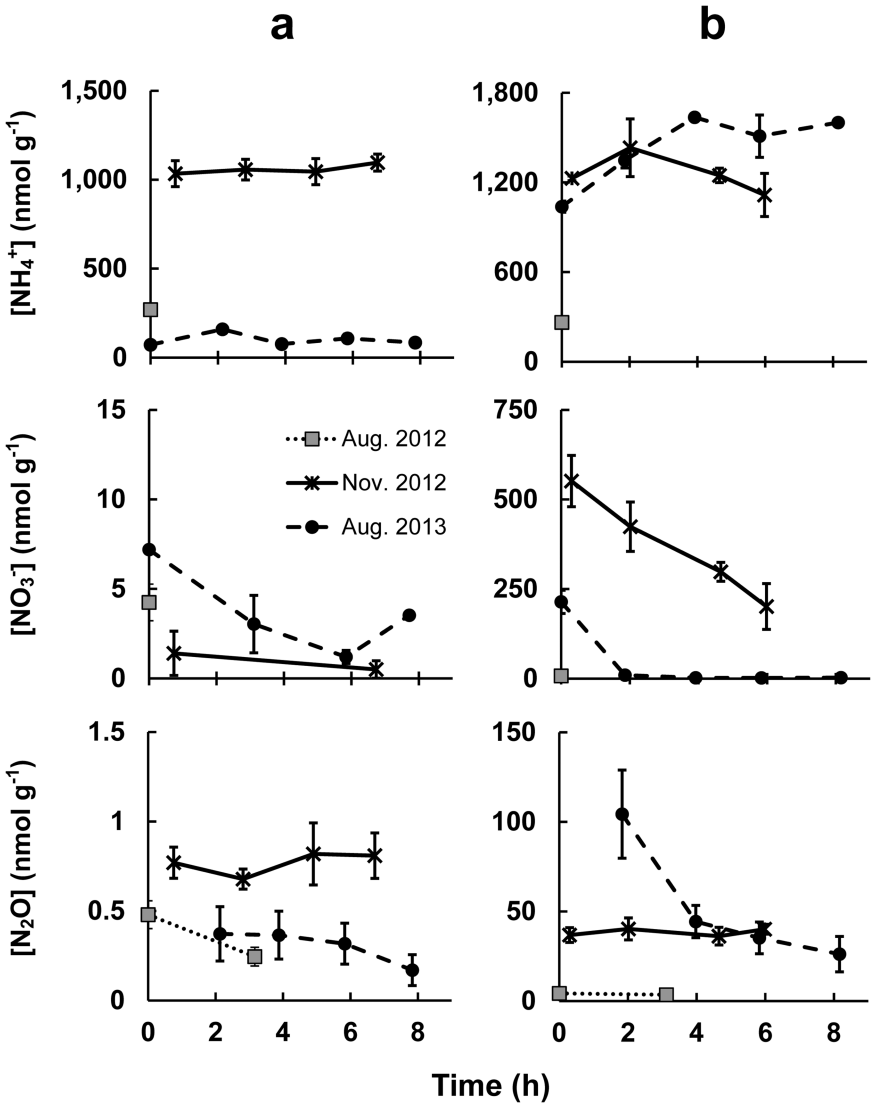

Figure 2. Time courses of NH_4^+, NO_3^-, and N_2O concentrations during incubation experiments of C and XF sediments under atmospheric oxygen headspace. The concentrations of NH_4^+, NO_3^-, and N_2O in sediment are normalized to one gram of wet sediment. Time zero indicates the moment of adding tracer solutions. (a) C sediment; (b) XF sediment. NH_4^+, NO_3^-, and N_2O concentrations are shown in upper, middle, and lower panels, respectively.

NH_4^+ concentration showed a net increase after 8 hours. XF generally had higher initial NO_3^- concentrations than C. Sediments from both C and XF plots that were incubated under atmospheric oxygen level had significant decreases in NO_3^- concentrations, suggesting active denitrification. Net NO_3^- consumption rates ranged from ~0.1 nmol N g^{-1} h^{-1} in C from August 2013 to ~80 nmol N g^{-1} h^{-1} in XF from November 2012 and even higher (>100 nmol N g^{-1} h^{-1}) during the first 2 hours of incubation in XF from August 2013. Changes in N_2O concentration with time displayed different patterns with season. In November 2012, neither C nor XF incubations had significant change ($P > 0.1$, ANOVA) in N_2O concentrations, whereas in August 2013, N_2O concentrations decreased in both incubations. In the shorter incubation (3 hours) from August 2012, N_2O concentration decreased, but the trend was less pronounced.

c. Change of $^{15}N - N_2O$ with time in ^{15}N-NH_4 and ^{15}N-NO_3 treatments during incubations of C and XF in November 2012

N_2O concentration did not change significantly in C and XF sediment; however, the increase in $^{15}N_2O$ indicates N_2O production. In ^{15}N-NH_4^+ treatments in November 2012, ^{15}N-N_2O increased in both C and XF (middle panels of Fig. 3a and b). In ^{15}N-NO_3 treatments, ^{15}N-N_2O also increased in XF. In C ^{15}N-NO_3 treatments, however, the ^{15}N-N_2O pool was already enriched to 0.398 atom % (natural abundance = 0.367 atom %) at 30 minutes, but ^{15}N-N_2O then decreased from 30 minutes to the end of the incubation (middle panels of Fig. 3a and b).

Both of these ^{15}N-N_2O patterns in ^{15}N-NO_3^- treatments were also observed in other incubation experiments (Fig. S2b in the supplementary material), with low sediment NO_3^- concentration correlating with decreasing ^{15}N-N_2O and vice versa.

d. Modeled N_2O production rates

Model simulations of N_2O concentrations and N_2O isotope data were used to derive the N_2O production and consumption rates (Fig. 4). Even though there was no significant change in N_2O concentration in some cases (e.g., C and XF from November 2012 in Fig. 3), simultaneous N_2O production and consumption occurred in all experiments.

N_2O production rates from NH_4^+ were 0.05 ± 0.01 and 0.9 ± 0.1 nmol N g^{-1} h^{-1} in August 2012 C and XF sediment, respectively (Fig. 4a). N_2O production from NO_3^- was greater than that from NH_4^+; rates were 0.2 ± 0.02 and 1.5 ± 0.2 nmol N g^{-1} h^{-1} in C and XF sediment, respectively. In November 2012, N_2O production rates from XF sediments ranged from 1.7 nmol N g^{-1} h^{-1} in XF-t to 55 nmol N g^{-1} h^{-1} in XF-d (Fig. 4b), one to two orders of magnitude higher than C, LF, and HF sediments, in which rates were generally <0.15 nmol N g^{-1} h^{-1} (Fig. 4c). When NO_3^- was present at low to undetectable concentrations (C, LF, and HF), N_2O production was dominated by NH_4^+ oxidation; when NO_3^- was abundant (XF, XF-d, and XF-m), N_2O production rates from NO_3^- were 12–42 nmol N g^{-1} h^{-1}, 3 to 15 times higher than N_2O production rates from NH_4^+, indicating

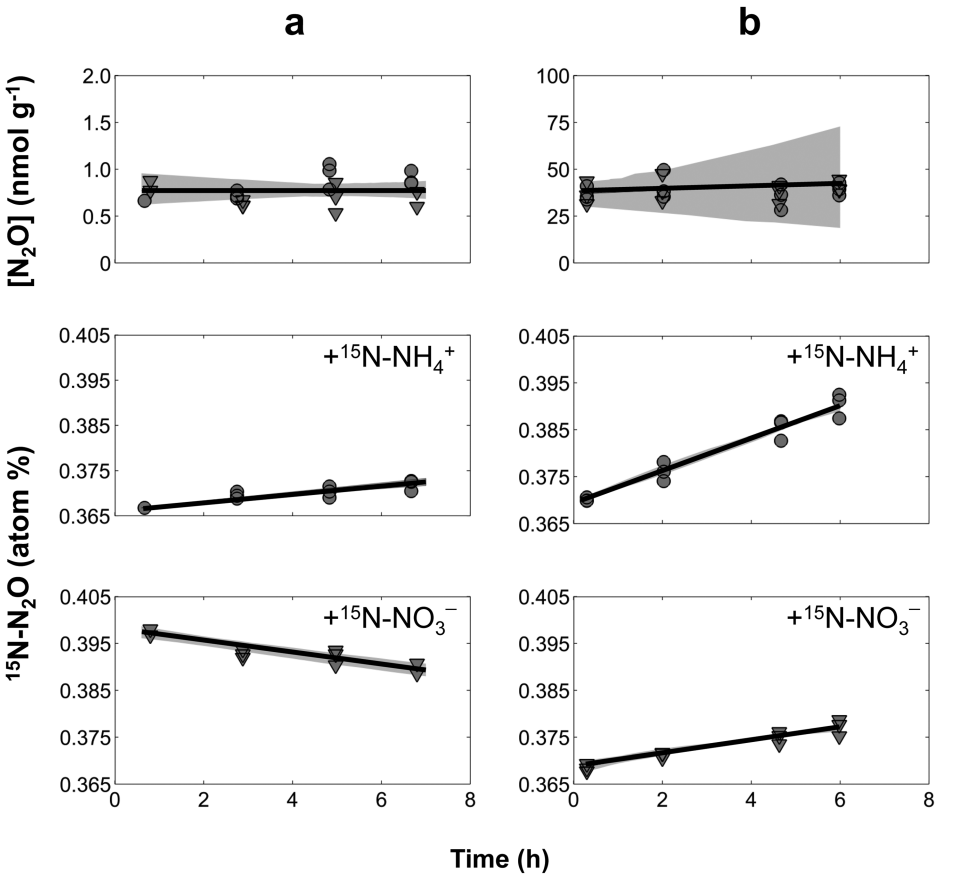

Figure 3. Time courses of N_2O concentration and ^{15}N-N_2O during incubation experiment under oxygenated headspace. Time zero indicates the moment of adding tracer solutions. (a) C sediment from November 2012. (b) XF sediment from November 2012. Filled circles (from ^{15}N-NH_4^+ treatment) and triangles (from ^{15}N-NO_3^- treatment) represent measurements; solid lines represent "best fit" of model simulation; shaded areas represent 95% confidence band for model simulations. Evolution of N_2O concentration in sediment is shown in the upper two panels; ^{15}N-N_2O evolution in ^{15}N-NH_4 treatment and ^{15}N-NO_3 treatment is shown in the middle and lower panels, respectively. See Figure S3 (in the supplementary material) for the complete set of model simulations.

denitrification as the major production pathway. In XF-t where NO_3^- was low (~3 nmol g^{-1}; Fig. S1 in the supplementary material) throughout the incubation period, unlike the other XF samples, N_2O production from NO_3^- was very low (<0.05 nmol N g^{-1} h^{-1}), and NH_4^+ was the dominant source of N_2O, with a production rate of 1.7 ± 0.1 nmol N g^{-1} h^{-1}. In August 2013 (Fig. 4d), XF sediment had much higher N_2O production rates than C and HF sediments. XF sediment had an initial NO_3^- concentration of 214 nmol g^{-1}, but the

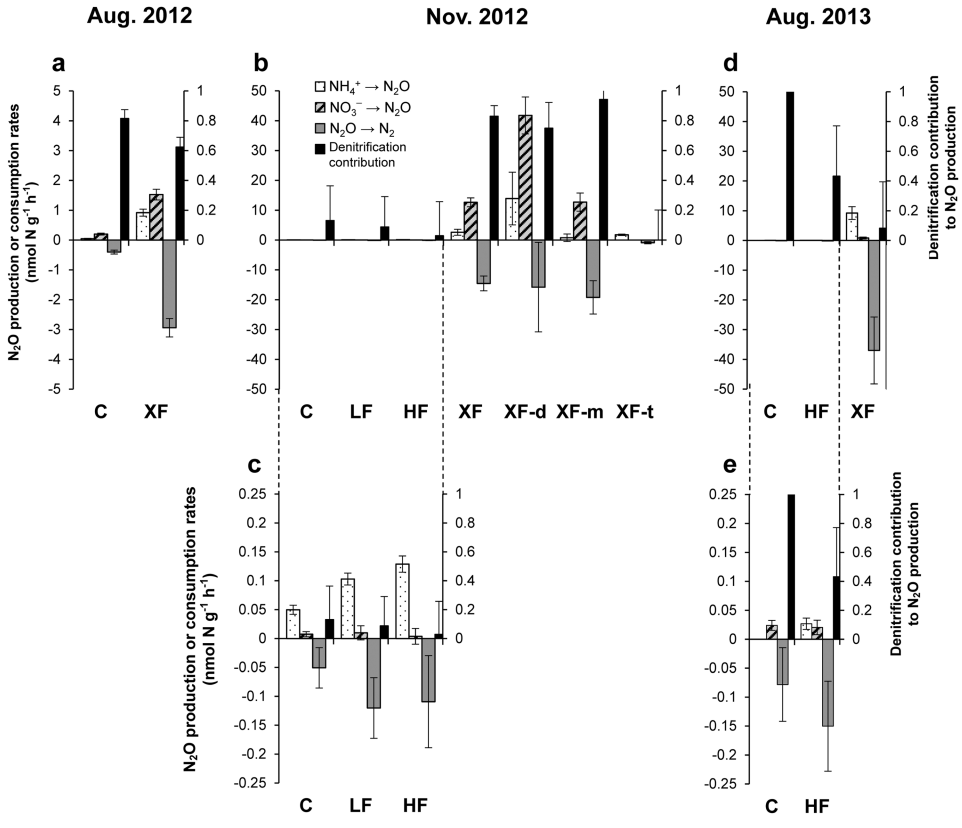

Figure 4. Modeled N_2O production rates from NH_4^+ (dotted bars), N_2O production rates from NO_3^- (striped bars), N_2O consumption rates (gray bars), and contribution of denitrification to total N_2O production (black bars, scale on the right). Note that N_2O consumption rates are presented as negative values. (A) Sediment collected in August 2012. (B) Sediment collected in November 2012. (C) Rates of N2O production and consumption and denitrification contribution in C, LF and HF incubations from November 2012. (D) Sediment collected in August 2013. (E) C, HF incubations from August 2013. Error bars represent Monte Carlo simulation (n = 10,000) derived standard deviations.

concentration dropped significantly to <3 nmol g^{-1} in the first 2 hours of incubation and maintained a low NO_3^- concentration for the remainder of the incubation (Fig. 2b, middle panel). Thus, from 2 hours onward, nitrification became the major N_2O production pathway, at a rate of 11.7 nmol N g^{-1} h^{-1}. N_2O production was mainly from NO_3^- in C at a rate of <0.03 nmol N g^{-1} h^{-1}. Similar N_2O production rates occurred in HF, where both NH_4^+ and NO_3^- served as nitrogen sources (Fig. 4e).

N_2O production rates from NH_4^+ and NO_3^- were used to calculate relative contributions of nitrification and denitrification to N_2O production. The fraction of N_2O produced from denitrification in each experiment is shown in Figure 4. Except for C sediment collected in August 2013, all samples showed N_2O production from NH_4^+. In C, LF, HF, and XF-t sediment from November 2012, where NO_3^- was low or undetectable, NH_4^+ was the major nitrogen source. When NO_3^- was present (>3 nmol g^{-1}), for example, in XF, XF-d, and XF-m from November 2012, the majority of N_2O was produced from NO_3^-.

e. Modeled N_2O consumption rates and the effect of oxygen on N_2O and NO_3^- consumption

It is interesting to note that net N_2O consumption occurred in some incubations under atmospheric oxygen headspace, as shown by decreasing N_2O concentration (Fig. 2, lower panels; and Fig. S3 in the supplementary material). Sediments collected in August 2012 and 2013 showed greater N_2O consumption than production (Fig. 4a and d). N_2O consumption rates in November 2012 sediments were generally similar to or lower than production rates (Fig. 4b and c). N_2O consumption rates were higher in XF than in other plots; the lowest was 1 nmol N g^{-1} h^{-1} (XF-t from November 2012), and the peak was at ~40 nmol N g^{-1} h^{-1} in XF from August 2013. N_2O consumption rates for C, LF, and HF were generally <0.2 nmol N g^{-1} h^{-1}, one to two orders of magnitude lower than XF.

The subset of XF sediment from November 2012 incubated under helium headspace was compared with incubations under oxygenated headspace (Fig. 5). In helium headspace ($-O_2$) incubations, after NO_3^- depletion, N_2O concentration decreased significantly to <5 nmol g^{-1} between 2.3 and 4.8 h, at a rate of ~25 nmol N g^{-1} h^{-1} (Fig. 5, upper panel). Lower N_2O consumption rate (~15 nmol N g^{-1} h^{-1}) was modeled when incubated with atmospheric oxygen ($+O_2$) in the presence of NO_3^-. No significant changes occurred in N_2O concentrations (Fig. 5, lower panel).

4. Discussion

Salt marsh sediment is potentially a net N_2O source to the atmosphere via nitrification and denitrification. These microbial processes depend on availabilities of NH_4^+ and NO_3^- for nitrogen sources. Because NH_4^+ oxidation requires oxygen and NO_3^- reduction does not, strong redox gradients in the sediment allow N_2O production via NH_4^+ oxidation, NO_3^- reduction to N_2O, and N_2O consumption to co-occur. In Great Sippewissett Marsh,

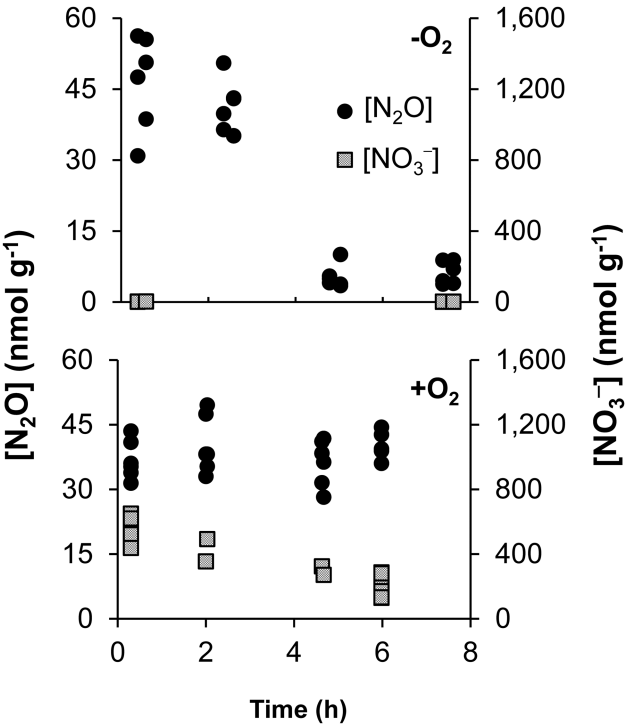

Figure 5. Time courses of N_2O and NO_3^- concentrations during incubation experiment for XF sediment from November 2012, under low oxygen and atmospheric headspaces. Upper panel: headspace purged with helium to remove oxygen (labeled "$-O_2$"); lower panel: atmospheric oxygen headspace (labeled "$+O_2$"). The concentrations of NO_3^- and N_2O in sediment are normalized to one gram of wet sediment.

sediment has been subjected to long-term fertilization, resulting in elevated N_2O production and consumption rates.

a. Inorganic nitrogen availability controls nitrogen sources for N_2O production

Results from incubation experiments showed that when NO_3^- concentration was low or undetectable (e.g., C, LF, HF, and XF-t from November 2012), NH_4^+ was the dominant nitrogen substrate for N_2O production, supported by the increase of ^{15}N-N_2O in ^{15}N-NH_4^+ treatments (Fig. 3a). In ^{15}N-NO_3^- treatments, the decrease of ^{15}N-N_2O from initial ^{15}N enrichment indicated that NH_4^+, which was not labeled with ^{15}N, contributed nitrogen to N_2O. Model simulations confirmed that NH_4^+ oxidation alone could explain the progressive enrichment of N_2O with ^{15}N in ^{15}N-NH_4^+ treatments, as well as dilution by ^{14}N from unlabeled NH_4^+ in ^{15}N-NO_3^- treatments (Fig. 3a). When NO_3^- was present throughout the incubation experiment, for example, XF, XF-d, and XF-m sediment from November 2012

where NO_3^- >500 nmol g^{-1} (Table 2), both NO_3^- and NH_4^+ were nitrogen substrates for N_2O production, as indicated by simultaneous increase in ^{15}N-N_2O in both ^{15}N-NH_4^+ and ^{15}N-NO_3^- treatments (Fig. 3b). Model simulation showed that the major nitrogen source compound for N_2O was NO_3^-, presumably as a consequence of active denitrification, consistent with the observed decrease in NO_3^- concentration (Fig. 2b).

The nitrogen substrate determination provides insights into N_2O production pathways. As a product of heterotrophic remineralization, NH_4^+ was always present at high concentrations (>70 nmol g^{-1}). In sediment with low NO_3^- concentrations, such as C, LF, and HF sediments, NH_4^+ was the major substrate for N_2O production. Thus, it appears that the N_2O production pathways supported by NH_4^+ oxidation, such as nitrifier denitrification and coupled nitrification-denitrification (Wrage et al. 2001), are responsible. NO_3^- could be supplied by fertilizer or potentially by nitrification (Kaplan, Valiela, and Teal 1979), or from groundwater discharge (Valiela and Teal 1979). Current incubation experiments showed denitrification was responsible for the majority of N_2O production in sediments with high NO_3^- concentration (~500 nmol g^{-1}), despite NH_4^+ being the major form of inorganic nitrogen. This suggests that NO_3^- availability may be an indicator of N_2O production pathways in these sediments, consistent with short-term NO_3^- addition stimulating N_2O emission as reported by Moseman-Valtierra et al. (2011). Further research could investigate the relative physiological advantage between nitrification and denitrification in these sediments under different NO_3^- availabilities to test how N_2O production pathways are regulated.

b. The control of N_2O production and consumption by oxygen

Oxygen concentration, which is spatially and temporally variable in tidal marshes, regulates N_2O production and consumption. When incubated under atmospheric oxygen headspace, NH_4^+ oxidation, NO_3^- reduction, and N_2O consumption were detected. In XF sediment from November 2012, N_2O production was balanced by consumption, as indicated by no significant change in headspace N_2O concentrations over the course of the incubation. The significant decrease in N_2O concentration under low oxygen conditions suggested elevated N_2O consumption and decreased N_2O production, because once oxygen was removed from the headspace, NH_4^+ oxidation ceased so that NO_3^- became the only possible nitrogen source for N_2O production. As nitrification ceased and thus no more NO_3^- was produced, denitrification resulted in a net loss of NO_3^-, and eventually NO_3^- was depleted. Greater net consumption of N_2O followed because (1) there was no NH_4^+ oxidation producing N_2O, (2) depletion of NO_3^- prevented an additional N_2O source, and (3) N_2OR was relieved from oxygen inhibition; this was confirmed by the elevated N_2O consumption rate discussed in Section 3e.

As the plants' roots penetrate deeper than 10 cm, sediments collected for incubation experiments are likely to experience molecular oxygen supplied from tidal water as well as diffusion from air. In August, actively growing *S. alterniflora* oxidizes the sediment (Howes et al. 1981), potentially favoring the growth of aerobes and aerobic metabolism.

Because incubation experiments were performed in a closed system with limited oxygen, such active aerobic processes would lower the oxygen concentration in sediment, allowing N_2O consumption to occur. This could be the reason that N_2O consumption exceeded production during incubation in August (Fig. 4a, d, and e). In November, growth of *S. alterniflora* ceases and in situ remineralization supports the growth of denitrifiers. When incubation was performed in the absence of oxygen, NO_3^- and N_2O were consumed in a few hours, indicating the presence of active denitrifiers. When oxygen was present in the headspace, oxygen inhibition of N_2OR decreased N_2O consumption rates. Further studies focused on the effects of oxygen availability on activities of nitrifiers and denitrifiers on a tidal cycle as well as seasonal cycle would provide more insight into N_2O fluxes in these time frames.

c. Nitrogen loading affects the N_2O production rates

As demonstrated in this study, increased N_2O production and consumption rates correlate with nitrogen loading from fertilizer. This is probably because fertilizer input enhances plant growth, and subsequent accumulation of above- and belowground biomass provides nutrients and electron donors to support nitrogen metabolisms, including denitrification (Hamersley and Howes 2005; Koop-Jakobsen and Giblin 2010). It should be noted that intermediate nitrogen loading (LF and HF plots), though already higher than the nitrogen loading of the vast majority of New England salt marshes, did not significantly increase sediment N_2O concentrations. Only XF plots, where the nitrogen loading is more than 40 times higher than background, showed significantly elevated N_2O concentrations. This indicates that elevated nitrogen loading at low to intermediate levels does not necessarily enhance N_2O production. Thus, denitrification is likely important in the consumption of N_2O. This is consistent with the finding of Lee et al. (1997) who showed that the emission ratio of N_2O:N_2 in marsh sediment is lower under higher nitrogen loading and called for future studies targeting the variability of N_2O:N_2 emissions in salt marsh sediment.

Increasing nitrogen loading from fertilization also resulted in changes in the relative contribution from NH_4^+ versus NO_3^- to N_2O production. Fertilization results in higher NO_3^- availability from fertilizer and possibly from NH_4^+ oxidation, thus increasing NO_3^- availability to support NO_3^- reduction to N_2O. As N_2O yield during denitrification is generally higher than that of nitrification (Bange 2008), it is likely that NO_3^- reduction to N_2O becomes the major production pathway when denitrification occurs. This was observed in XF plots except XF-t from November 2012. In sediments with low fertilizer supply and in XF-t from November 2012, NH_4^+ was the dominant inorganic nitrogen form and NO_3^- was present at low concentration because of rapid turnover by denitrification and tidal efflux (Brin et al. 2010). Therefore, the majority of N_2O was produced via NH_4^+ oxidation. Unlike all other XF samples, XF-t behaved more like the lower fertilized samples. NO_3^- concentration was low in XF-t in November 2012 possibly because of its lower elevation, which is subjected to

more frequent tidal exchange. Thus, N_2O production was dominated by NH_4^+ oxidation; the production and consumption rate ($\sim$1 nmol N g^{-1} h^{-1}) was an order of magnitude higher than rates in lower fertilization plots ($\sim$0.1 nmol N g^{-1} h^{-1}).

Studies conducted in New England salt marshes (e.g., Great Sippewissett Marsh and Plum Island Estuary) have shown that decadal-scale elevated fertilizer input promotes the removal of excess nitrogen via denitrification (Hamersley and Howes 2005; Koop-Jakobsen and Giblin 2010). However, many adverse effects are reported, such as increasing NO_3^- export to the adjacent estuary (Brin et al. 2010), subsidence of marsh surface because of reduction of organic matter accumulation (Turner et al. 2009), loss of marsh coverage because of reduced stability of sediment-root matrices and sea-level rise (Deegan et al. 2012), and greater N_2O production, as demonstrated in this study.

d. Factors in interpretation of experimental and model results in the actual environment

Homogenization of the sediment for these incubation experiments greatly altered the conditions to which organisms were exposed. Because this disruption occurred in all experiments, it should not obscure the treatment effect of different fertilizer levels. During the handling of sediment, availabilities of inorganic nitrogen might have changed because of active nitrification and denitrification. Exposing the sediment under atmospheric oxygen headspace may have partially inhibited denitrifiers, leading to underestimation of the reduction of NO_3^- or N_2O, as well as overestimation of nitrification. Despite homogenization in atmospheric oxygen, however, both nitrifiers and denitrifiers were apparently still active in the incubations, as shown by the simultaneous increase of ^{15}N-N_2O in both ^{15}N-NH_4^+ and ^{15}N-NO_3^- treatments (Fig. 3b). Thus, ^{15}N tracer incubation experiments identified potential pathways and rates for N_2O production and consumption. Also, incubation with homogenized sediment allowed the isolation of the intercorrelated variables, such as fertilization, plant biomass, and sediment inorganic nitrogen levels, which was necessary to discern the dependence of N_2O production on environmental factors.

The model simulation in this study is capable of distinguishing nitrogen source compounds for N_2O production but cannot determine the exact biochemical pathways involved. Even though there was coupling between nitrification and denitrification, during which nitrogen was transferred from NH_4^+ to NO_3^- and to N_2O, the data did not specify the pathway by which the transfer occurred. It may be possible in the future to use the dual isotope approach, combining ^{18}O as another tracer to identify the pathways (Kool, Van Groenigen, and Wrage 2011). The model parameterization in this study, using constant N_2O production and consumption rates, adequately described the majority of the experimental data. However, NH_4^+ oxidation, NO_3^- reduction, and N_2O reduction are enzymatic processes, often assumed to follow Michaelis-Menten kinetics. The use of concentration-dependent nitrogen transformation rates may simulate the observations more accurately in the few incubations in which concentrations changed appreciably, notably the XF experiment in August 2013. In this experiment, the N_2O concentration decreased, which probably caused the rate of N_2O

consumption to decrease, and this was poorly represented by concentration-independent modeled rates (Fig. S3 in the supplementary material).

In C sediment from November 2012, N_2O was rapidly (i.e., by the first time point) enriched with ^{15}N in the $^{15}NO_3$ treatment, whereas there was no initial ^{15}N enrichment of N_2O observed in the ^{15}N-NH_4^+ treatment. Similar observations have been reported by Stevens et al. (1997), who attributed such phenomena to $^{15}NO_2^-$ impurity in $^{15}NO_3^-$ tracer, and $^{15}NO_2^-$ rather than $^{15}NO_3^-$ underwent rapid chemical reduction to N_2O. However, the amount of $^{15}NO_2^-$ impurity in the $^{15}NO_3^-$ tracer used in this study was 80 ppm, which was not sufficient to enrich the initial ^{15}N-N_2O to the observed level. The reason for this initial enrichment was not fully understood and requires further investigation.

Potential rates of N_2O production from NH_4^+ and NO_3^- under controlled environmental conditions were shown in this study. To further investigate in situ N_2O production in natural salt marshes, nonintrusive methods such as in situ incubations coupled with flux chambers (Moseman-Valtierra et al. 2011), or evaluation of N_2O isotopic signatures from different production pathways, would be necessary.

5. Conclusion

Coastal salt marshes play an important role in the removal of land-derived excess nitrogen via several microbial processes that produce N_2O. Using ^{15}N tracer incubations and numerical modeling, the availabilities of inorganic nitrogen and oxygen and nitrogen loading were the controlling factors of N_2O production and consumption. NO_3^- was the major nitrogen substrate for N_2O production under high NO_3^- concentrations, and NH_4^+ was the dominant nitrogen source under low NO_3^- concentrations. Oxygen was critical in regulating N_2O consumption, which was enhanced in incubations under anoxic headspace. Decadal-scale fertilization increased sediment NH_4^+ and NO_3^- concentrations; plots with the highest fertilization had significantly higher rates of N_2O production and consumption than control. Therefore, increasing anthropogenic nitrogen loading will increase nitrogen substrate availabilities and nitrogen transformation rates, and thus, N_2O flux from salt marshes is likely to increase. Short-term, high fluxes of N_2O are possible if N_2O production and consumption decouple as a consequence of coastal eutrophication.

Acknowledgments. The authors are indebted to the owners of salt marsh parcels, Salt Pond Sanctuaries and Dr. E. F. X. Hughes, for allowing us to have access to the experimental plots within their properties. We gratefully acknowledge those responsible for the establishment of the long-term experimental plots, which made these experiments possible. The fertilization experiment at the Great Sippewissett Marsh started with a collaboration between Ivan Valiela and John Teal. In recent years, Brian Howes and Dale Goehringer have maintained the fertilization plots, with funding support from the National Science Foundation (NSF; OCE-0453292, DEB-0516430 to I. Valiela). The authors thank John Angell and Patrick Kearns for their support during sample collection.

In the preparation of this manuscript, the authors acknowledge Frederik Simons for significant advice on numerical modeling and optimization, and François Morel and Daniel Sigman for their

helpful advice and discussions on this manuscript. The manuscript was greatly improved by suggestions from two anonymous reviewers. This work was funded by the NSF (DEB-1019624 to BBW and JLB).

REFERENCES

Arp, D. J., and L. Y. Stein. 2003. Metabolism of inorganic N compounds by ammonia-oxidizing bacteria. Crit. Rev. Biochem. Mol. Biol., *38*(6), 471–495.

Bange, H. W. 2008. Gaseous nitrogen compounds (NO, N_2O, N_2, NH_3) in the ocean, *in* Nitrogen in the Marine Environment, 2nd ed., D. G. Capone, D. A. Bronk, M. R. Mulholland, and E. J. Carpenter, eds. Burlington, MA: Academic Press, 51–94.

Bange, H. W., S. Rapsomanikis, and M. O. Andreae. 1996. Nitrous oxide in coastal waters. Global Biogeochem. Cycles, *10*(1), 197–207.

Blackwell, M. S. A., S. Yamulki, and R. Bol. 2010. Nitrous oxide production and denitrification rates in estuarine intertidal saltmarsh and managed realignment zones. Estuarine, Coastal Shelf Sci., *87*(4), 591–600.

Bonin, P., M. Gilewicz, and J. C. Bertrand. 1989. Effects of oxygen on each step of denitrification on *Pseudomonas nautica*. Can. J. Microbiol., *35*(11), 1061–1064.

Bowen, J. L., J. E. K. Byrnes, D. Weisman, and C. Colaneri. 2013. Functional gene pyrosequencing and network analysis: An approach to examine the response of denitrifying bacteria to increased nitrogen supply in salt marsh sediments. Front. Microbiol., *4*, 342. doi: 10.3389/fmicb.2013.00342

Bowen, J. L., and I. Valiela. 2001. Historical changes in atmospheric nitrogen deposition to Cape Cod, Massachusetts, USA. Atmos. Environ., *35*(6), 1039–1051.

Braman, R. S., and S. A. Hendrix. 1989. Nanogram nitrite and nitrate determination in environmental and biological materials by vanadium(III) reduction with chemiluminescence detection. Anal. Chem., *61*(24), 2715–2718.

Brin, L. D., I. Valiela, D. Goehringer, and B. Howes. 2010. Nitrogen interception and export by experimental salt marsh plots exposed to chronic nutrient addition. Mar. Ecol.: Prog. Ser., *400*, 3–17.

Cicerone, R. J. 1987. Changes in stratospheric ozone. Science, *237*(4810), 35–42.

Crutzen, P. J. 1970. The influence of nitrogen oxides on the atmospheric ozone content. Q. J. R. Meteorol. Soc., *96*(408), 320–325.

Dawson, T. E., and R. T. W. Siegwolf. 2007. Using stable isotopes as indicators, tracers, and recorders of ecological change: Some context and background, *in* Terrestrial Ecology, Vol. 1, Stable Isotopes as Indicators of Ecological Change, T. E. Dawson and R. T. W. Siegwolf, eds. Amsterdam: Elsevier, 1–18.

Deegan, L. A., D. S. Johnson, R. S. Warren, B. J. Peterson, J. W. Fleeger, S. Fagherazzi, and W. M. Wollheim. 2012. Coastal eutrophication as a driver of saltmarsh loss. Nature, *490*, 388–392.

Fox, L., I. Valiela, and E. L. Kinney. 2012. Vegetation cover and elevation in long-term experimental nutrient-enrichment plots in Great Sippewissett salt marsh, Cape Cod, Massachusetts: Implications for eutrophication and sea level rise. Estuaries Coasts, *35*(2), 445–458.

Garside, C. 1982. A chemiluminescent technique for the determination of nanomolar concentrations of nitrate and nitrite in seawater. Mar. Chem., *11*(2), 159–167.

Hamersley, M. R., and B. L. Howes. 2005. Coupled nitrification–denitrification measured in situ in a *Spartina alterniflora* marsh with a $^{15}NH_4^+$ tracer. Mar. Ecol.: Prog. Ser., *299*, 123–135.

Hamlett, N. V. 1986. Alteration of a salt marsh bacterial community by fertilization with sewage sludge. Appl. Environ. Microbiol., *52*, 915–923.

Howes, B. L., J. W. H. Dacey, and D. D. Goehringer. 1986. Factors controlling the growth form of *Spartina alterniflora*: Feedbacks between above-ground production, sediment oxidation, nitrogen and salinity. J. Ecol., *74*(3), 881–898.

Howes, B. L., R. W. Howarth, J. M. Teal, and I. Valiela. 1981. Oxidation-reduction potentials in a salt marsh: Spatial patterns and interactions with primary production. Limnol. Oceanogr., *26*(2), 350–360.

Intergovernmental Panel on Climate Change (IPCC). 2013. Carbon and other biogeochemical cycles, *in* Climate Change 2013: The Physical Science Basis. Contribution of Working Group I to the Fifth Assessment Report of the Intergovernmental Panel on Climate Change, T. F. Stocker, D. Qin, G.-K. Plattner, M. Tignor, S. K. Allen, J. Boschung, A. Nauels, Y. Xia, V. Bex, and P. M. Midgley, eds. Cambridge, UK: Cambridge University Press, 465–570.

Kaplan, W., I. Valiela, and J. M. Teal. 1979. Denitrification in a salt marsh ecosystem. Limnol. Oceanogr., *24*(4), 726–734.

Kinney, E. L., and I. Valiela. 2013. Changes in $\delta^{15}N$ in salt marsh sediments in a long-term fertilization study. Mar. Ecol.: Prog. Ser., *477*, 41–52.

Kool, D. M., J. W. Van Groenigen, and N. Wrage. 2011. Source determination of nitrous oxide based on nitrogen and oxygen isotope tracing: dealing with oxygen exchange, *in* Methods in Enzymology, Vol. 496, Research on Nitrification and Related Processes, Part B, M. G. Klotz and L. Y. Stein, eds. Burlington, MA: Academic Press, 139–160.

Koop-Jakobsen, K., and A. E. Giblin. 2010. The effect of increased nitrate loading on nitrate reduction via denitrification and DNRA in salt marsh sediments. Limnol. Oceanogr., *55*(2), 789–802.

Körner, H., and W. G. Zumft. 1989. Expression of denitrification enzymes in response to the dissolved oxygen level and respiratory substrate in continuous culture of *Pseudomonas stutzeri*. Appl. Environ. Microbiol., *55*(7), 1670–1676.

Lee, R. Y., S. B. Joye, B. J. Roberts, and I. Valiela. 1997. Release of N_2 and N_2O from salt-marsh sediments subject to different land-derived nitrogen loads. Biol. Bull., *193*, 292–293.

Moseman-Valtierra, S. 2012. Reconsidering climatic roles of marshes: Are they sinks or sources of greenhouse gases? *in* Marshes: Ecology, Management and Conservation, D. C. Abreu and S. L. de Borbón, eds. New York: Nova Science, 1–48.

Moseman-Valtierra, S., R. Gonzalez, K. D. Kroeger, J. Tang, W. C. Chao, J. Crusius, J. Bratton, A. Green, and J. Shelton. 2011. Short-term nitrogen additions can shift a coastal wetland from a sink to a source of N_2O. Atmos. Environ., *45*(26), 4390–4397.

Pérez, T. 2005. Factors that control the isotopic composition of N_2O from soil emissions, *in* Stable Isotopes and Biosphere-Atmosphere Interactions, L. B. Flanagan, J. R. Ehleringer, and D. E. Pataki, eds. San Diego, CA: Academic Press, 69–84.

Ravishankara, A. R., J. S. Daniel, and R. W. Portmann. 2009. Nitrous oxide (N_2O): The dominant ozone-depleting substance emitted in the 21st century. Science, *326*(5949), 123–125.

Santoro, A. E., C. Buchwald, M. R. McIlvin, and K. L. Casciotti. 2011. Isotopic signature of N_2O produced by marine ammonia-oxidizing archaea. Science, *333*(6047), 1282–1285.

Schilt, A., M. Baumgartner, T. Blunier, J. Schwander, R. Spahni, H. Fischer, and T. F. Stocker. 2010. Glacial–interglacial and millennial-scale variations in the atmospheric nitrous oxide concentration during the last 800,000 years. Quat. Sci. Rev., *29*(1–2), 182–192.

Seitzinger, S. P., and C. Kroeze. 1998. Global distribution of nitrous oxide production and N inputs in freshwater and coastal marine ecosystems. Global Biogeochem. Cycles, *12*(1), 93–113.

Sigman, D. M., K. L. Casciotti, M. Andreani, C. Barford, M. Galanter, and J. K. Böhlke. 2001. A bacterial method for the nitrogen isotopic analysis of nitrate in seawater and freshwater. Anal. Chem., *73*(17), 4145–4153.

Stevens, R. J., R. J. Laughlin, L. C. Burns, J. R. M. Arah, and R. C. Hood. 1997. Measuring the contributions of nitrification and denitrification to the flux of nitrous oxide from soil. Soil Biol. Biochem., *29*(2), 139–151.

Strickland, J. D. H., and T. R. Parsons. 1968. A Practical Handbook of Seawater Analysis. Bulletin of Fisheries Research Board of Canada, no. 167. Ottawa, ON, Canada: Fisheries Research Board of Canada, 311 pp.

Turner, R. E., B. L. Howes, J. M. Teal, C. S. Milan, E. M. Swenson, and D. D. Goehringer-Toner. 2009. Salt marshes and eutrophication: An unsustainable outcome. Limnol. Oceanogr., *54*(5), 1634–1642.

Valiela, I., and J. M. Teal. 1979. The nitrogen budget of a salt marsh ecosystem. Nature, *280*(5724), 652–656.

Valiela, I., J. M. Teal, and W. Sass. 1973. Nutrient retention in salt marsh plots experimentally fertilized with sewage sludge. Estuarine Coastal Mar. Sci., *1*(3), 261–269.

Valiela, I., J. M. Teal, and W. J. Sass. 1975. Production and dynamics of salt marsh vegetation and the effects of experimental treatment with sewage sludge. Biomass, production and species composition. J. Appl. Ecol., *12*(3), 973–981.Wrage, N., G. L. Velthof, M. L. van Beusichem, and O. Oenema. 2001. Role of nitrifier denitrification in the production of nitrous oxide. Soil Biol. Biochem., *33*(12–13), 1723–1732.

Received: *19 August 2014*; revised: *7 April 2015*.